Program Digest, 2019 IEEE International Ultrasonics Symposium (IUS)
Glasgow, Scotland, October 6-9, 2019

Imaging of pulse wave propagation coupled with vector flow and wall shear stress mapping in atherosclerotic plaque phantoms and in vivo

Grigorios Marios Karageorgos
Department of Biomedical Engineering
Columbia University
New York, USA

Iason Zacharias Apostolakis
Department of Biomedical Engineering
Columbia University
New York, USA

Pierre Nauleau
Department of Biomedical Engineering
Columbia University
New York, USA

Vittorio Gatti
Department of Biomedical Engineering
Columbia University
New York, USA

Rachel Weber
Department of Biomedical Engineering
Columbia University
New York, USA

Julien Grondin
Department of Biomedical Engineering
Columbia University
New York, USA

Elisa E. Konofagou
Department of Biomedical Engineering
Department of Radiology
Columbia University
New York, USA

Abstract — **Methods used in clinical practice to diagnose and monitor atherosclerosis present limitations. It has been reported that atherosclerosis alters the mechanical properties of the arterial wall, while the stiffness of a plaque can provide information on its risk for rupture and stroke occurrence. Pulse Wave Imaging (PWI) is a non-invasive, ultrasound-based technique, which provides information on arterial wall stiffness by imaging the pulse wave propagation along an arterial segment. Wall shear stress has also been considered as one of the key cardiovascular parameters associated with vascular wall degeneration and atherosclerosis initiation. The aim of the present study is to integrate PWI with Vector Doppler and Wall Shear stress in a single ultrasound imaging modality, enabling thus simultaneous and co-localized imaging of distension pulse wave propagation and hemodynamics. The performance of the proposed technique was evaluated in two phantoms with embedded plaques presenting 50% and 70% degree of stenosis, as well as through CFD simulations. Moreover, initial feasibility was demonstrated in an atherosclerotic human carotid artery in-vivo. Simultaneous compliance and flow measurements in the same artery could thus be obtained which can be used to both assess and monitor progression of vascular disease.**

Keywords—Pulse wave velocity, wall shear stress, atherosclerosis, arterial wall stiffness,

I. INTRODUCTION

Carotid artery disease is a vascular disease characterized by reduction of the carotid artery luminal area due to the development of atherosclerotic plaques. Carotid artery disease progresses slowly often without presenting any symptoms, until it deprives blood supply to the brain, causing a stroke or transient ischemic attack. In the current clinical practice, there are no reliable biomarkers associated with early detection of this condition [1]. Moreover, the risk for stroke is primarily evaluated based on the degree of stenosis. This criterion is, however, not highly reliable, since low stenotic plaques may also cause damage [2].

It has been reported that atherosclerosis alters the mechanical properties of the affected vessel [3][4]. Aging and hypertension which are known as two of the primary causes of atherosclerosis have been associated with increased arterial wall stiffness [5][6]. Moreover, the mechanical properties of an atherosclerotic plaque can provide information on the presence of vulnerable components and thus its risk for rupture and stroke occurrence[7][8]. Ultrasound elasticity imaging techniques have been investigated as a tool to non-invasively characterize arterial wall properties [9][10][11][12][7], showing great promise in vascular disease diagnosis and monitoring.

Pulse wave velocity (PWV) is an important cardiovascular marker that is widely considered as an measure of arterial stiffness[13]. Pulse wave imaging (PWI) is a non-invasive ultrasound technique which provides a regional PWV estimate along an imaged segment of a large artery [14][15][16][17] [18][19][20]. PWI has been shown capable of monitoring the progression of focal vascular diseases such as atherosclerosis [21][22] and abdominal aortic aneurism[23] in mice, while a more recent study demonstrated its feasibility to differentiate among plaques with different degree of calcification in carotid artery disease patients[24].

Blood flow patterns and wall shear stress (WSS) have been reported to alter the mechanical properties of the arterial wall and often lead to vascular disease [25][26]. Moreover, there has been a wide research interest in the role of WSS as a factor of vulnerable plaque development and plaque destabilization. It is therefore desirable to develop an imaging

modality that provides simultaneous information both on arterial wall mechanical properties and WSS in order to more accurately investigate the interaction between hemodynamics and arterial wall structure, potentially leading to more efficient monitoring of vascular disease progression.

The aim of the present study was to couple PWI with vector flow and WSS imaging, in a single imaging modality, providing simultaneous and co-localized information both on distension pulse wave propagation and blood flow dynamics. The performance of the proposed technique was evaluated two phantoms with embedded plaques presenting 50% and 70% degree of stenosis, as well as through CFD simulations. Moreover, initial feasibility was demonstrated in the common carotid artery in an atherosclerotic patient.

II. Methods

A. Phantom & Simulation Study

Two PVA phantoms were created using a 3-D printed mold, mimicking atherosclerotic vessels with 50% and 70% maximum stenosis. The phantoms were placed inside a container and their two ends were mounted onto plastic fittings. The phantoms were then embedded in a surrounding medium of Porcine-skin gelatin. The plastic fittings were connected to a programmable physiological flow pump (Compuflow 1000, Shelley Medical Imaging technologies, Ontario, Canada) to apply a physiological carotid artery flow waveform, with an amplitude of 20 cm/s and pulse duration of approximately 0.4 s. The fluid described in [27], with nylon scattering particles, and viscosity of 4 mPas was employed. The container in which the phantoms were embedded was filled with water, and the ultrasound probe was attached to a positioner right above the gelatin surrounding medium. An ultrasound acquisition was performed at a 37.8 mm longitudinal segment of each phantom, with the plaque centered in the field of view (FOV).

FEBio [28] was employed to simulate the flow through the phantom lumen. The 3-D CAD model of the 3-D printed phantom geometry was converted to FE model, and meshed appropriately. Zero fluid velocity was imposed at the outermost surface of the lumen. The same flow waveform as the one generated by the programmable pump was imposed at the inlet of the phantom models, while zero flow resistance was set at the outlet. A slightly compressible Newtonian viscous fluid was used to simulate the blood mimicking liquid used for the phantom experiments with a mass density, shear viscosity and bulk modulus of 1060 kg/m^3, 0.004 Pa s and 2 GPa, respectively. Subsequently, the time waveforms of x- and y-flow velocity components at each node on the central 2-D slice of the phantom lumen were exported and then post-processed in Matlab R2017b.

B. In-Vivo Study

All procedures performed for the human study were approved by the Human Research Protection Office (HRPO) and Institutional Review Boards (IRBs) of Columbia University. The right common carotid of one atherosclerotic subject (Male, 62 y.o.) was scanned at the level of the carotid bulb, presenting low degree of stenosis (<50%).

C. Acquisition Setup

A Vantage 256 system (Verasonics, Kirkland, USA) was used to drive an L7-4 Linear array transducer with 128 elements, at a center frequency of 5 MHz and 60% bandwidth. A coherent compounding sequence involving the transmission of 5 plane waves in the case of the phantom study and 3 plane waves in the case of the in-vivo study was implemented at a pulse repetition frequency of 8333 Hz [29]. The RF sampling rate was at 20 MHz.

D. PWI post-processing

A similar methodology as in [29] was performed. The acquired RF data were beamformed by using a parallel Delay and Sum algorithm implemented in CUDA. A GPU accelerated implementation of the Sum-Table 1-D normalized cross-correlation method was applied on the RF data in order to estimate the axial wall displacements, and then normalized with the frame rate to obtain the axial velocities. Subsequently, the anterior and posterior arterial walls were manually segmented, and the time waveform of the axial wall velocity of each wall were obtained at each lateral position. The wall velocities of the posterior wall were subtracted from the ones of the anterior wall, obtaining thus a spatiotemporal map of the of the arterial wall distension.

E. Vector flow velocity and Wall Shear stress estimation.

The compounded RF frames were filtered using a singular value decomposition (SVD) filter in order to eliminate the contribution of wall tissue motion [30]. A 2-D cross correletion method [31] was then applied to the filtered RF signals in order to estimate the axial and lateral components of flow velocity. Subsequently, the borders between the arterial walls and lumen were segmented using a semi-automated segmentation algorithm presented in [21]. WSS was calculated using the formula:

$$\mathrm{WSS} = \mu * \frac{\partial v_t}{\partial r},$$

where v_t is the tangent component of the flow velocity vector to the wall at a small distance r (r<0.3 mm), and μ is the fluid viscosity, assumed to be 3.45 mPa s in the case of the human subject [32]. The axial wall velocity values estimated through the PWI post-processing methodology were used to move the wall segmentation lines accordingly, in order to maintain constant distance from the wall (r) during the cardiac cycle.

The simulated and measured WSS were spatially registered along the phantom's longitudinal axis in order to correspond to the same FOV, and were compared at the time frame corresponding to peak systole.

III. Results

Figure 1-(a) demonstrates the PWI coupled with vector flow imaging, with the axial wall velocities and flow velocity magnitudes color-coded and the 2-D flow velocity vectors overlaid onto the B-mode. Figure 1-(b) illustrates the PWI

coupled with WSS imaging, with both quantities color-coded with different colormaps and overlaid onto the B-mode. Good agreement was found between measured and simulated WSS at peak systole time frame (50% stenosis phantom: relative residual error (RRE) = 9%, correlation coefficient (CC) = 0.87. 70% stenosis phantom: RE = 15%, CC = 0.83).

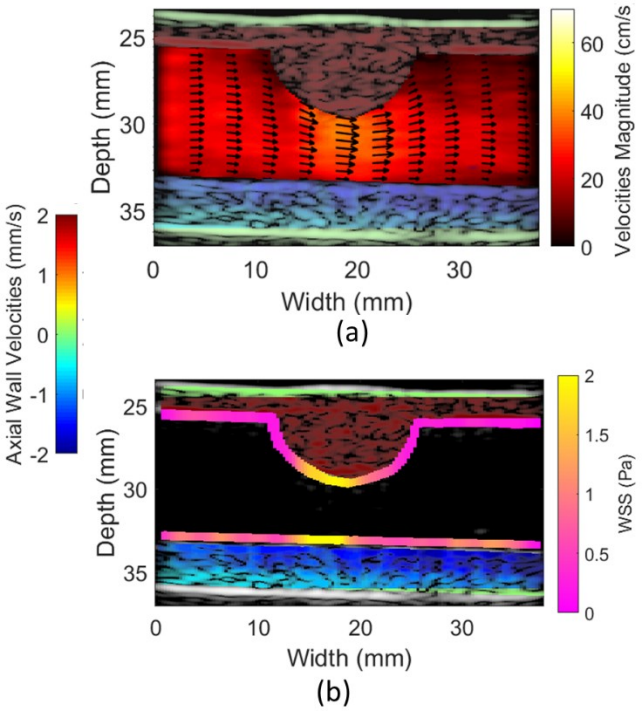

Figure. 1: Image sequences during peak systole in a vessel phantom with 50% stenosis (a) PWI coupled with vector flow imaging. (b) PWI coupled with WSS Imaging

In both phantoms, the highest WSS values were observed approximately at the positions of maximum stenosis (50% stenosis: 1.94 Pa, 70% stenosis: 3.54 Pa).

Figure 2 illustrates application of the proposed method in an atherosclerotic carotid artery in vivo, where WSS was elevated at plaque sites (Maximum WSS = 1.74 Pa).

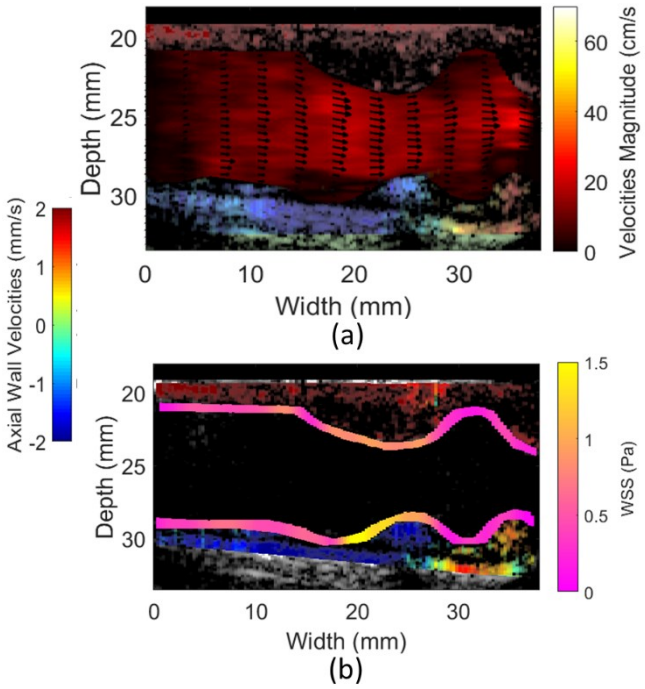

Figure. 2: Image sequences during peak systole in an atherosclerotic subject in-vivo (a) PWI coupled with vector flow imaging. (b) PWI coupled with WSS Imaging

IV. Conclusion

In conclusion, a method was presented that provides simultaneous and co-localized imaging of distension pulse wave propagation, vector flow and wall shear stress. The proposed method was validated through simulations and phantom experiments in two vessels presenting different degree of stenosis. Moreover, initial feasibility was demonstrated in an atherosclerotic common carotid artery in-vivo. The proposed method is expected to provide more insight in the interaction between blood flow dynamics and vessel wall properties, aiding thus in vascular disease diagnosis and monitoring.

Acknowledgment S

The study was funded in part by the National Institutes of Health: HL135734.

References

[1] A. Fernández-Ortiz *et al.*, "The Progression and Early detection of Subclinical Atherosclerosis (PESA) study: Rationale and design," *Am. Heart J.*, vol. 166, no. 6, pp. 990–998, Dec. 2013.

[2] T. Saam *et al.*, "The Vulnerable, or High-Risk, Atherosclerotic Plaque: Noninvasive MR Imaging for Characterization and Assessment," *Radiology*, vol. 244, no. 1, pp. 64–77, Jul. 2007.

[3] I. Z. Apostolakis, G. M. Karageorgos, P. Nauleau, S. D. Nandlall, and E. E. Konofagou, "Adaptive Pulse Wave Imaging: automated spatial vessel wall inhomogeneity detection in phantoms and in-vivo," *IEEE Trans. Med. Imaging*, pp. 1–1, 2019.

[4] W. W. Nichols, M. F. O'Rourke, C. Vlachopoulos, and D. A. McDonald, *McDonald's blood flow in arteries : theoretical, experimental and clinical principles.* Hodder Arnold, 2011.

[5] Z. Sun, "Aging, arterial stiffness, and hypertension.," *Hypertens.*

(Dallas, Tex. 1979), vol. 65, no. 2, pp. 252–6, Feb. 2015.

[6] A. P. Avolio, S. G. Chen, R. P. Wang, C. L. Zhang, M. F. Li, and M. F. O'Rourke, "Effects of aging on changing arterial compliance and left ventricular load in a northern Chinese urban community.," *Circulation*, vol. 68, no. 1, pp. 50–58, Jul. 1983.

[7] T. J. Czernuszewicz *et al.*, "Non-invasive in Vivo Characterization of Human Carotid Plaques with Acoustic Radiation Force Impulse Ultrasound: Comparison with Histology after Endarterectomy," *Ultrasound Med. Biol.*, vol. 41, no. 3, pp. 685–697, Mar. 2015.

[8] R. T. Lee *et al.*, "Prediction of mechanical properties of human atherosclerotic tissue by high-frequency intravascular ultrasound imaging. An in vitro study.," *Arterioscler. Thromb. A J. Vasc. Biol.*, vol. 12, no. 1, pp. 1–5, Jan. 1992.

[9] H. H. G. Hansen, G. J. de Borst, M. L. Bots, F. L. Moll, G. Pasterkamp, and C. L. de Korte, "Compound Ultrasound Strain Imaging for Noninvasive Detection of (Fibro)Atheromatous Plaques: Histopathological Validation in Human Carotid Arteries," *JACC Cardiovasc. Imaging*, vol. 9, no. 12, pp. 1466–1467, Dec. 2016.

[10] C. Schmitt, G. Soulez, R. L. Maurice, M.-F. Giroux, and G. Cloutier, "Noninvasive Vascular Elastography: Toward A Complementary Characterization Tool of Atherosclerosis in Carotid Arteries," *Ultrasound Med. Biol.*, vol. 33, no. 12, pp. 1841–1858, Dec. 2007.

[11] J. Garrard *et al.*, "Shear Wave Elastography May Be Superior to Greyscale Median for the Identification of Carotid Plaque Vulnerability: A Comparison with Histology," *Ultraschall der Medizin - Eur. J. Ultrasound*, vol. 36, no. 04, pp. 386–390, Jun. 2015.

[12] A. Bertrand-Grenier *et al.*, "Abdominal aortic aneurysm follow-up by shear wave elasticity imaging after endovascular repair in a canine model Abbreviations AAA Abdominal aortic aneurysm CEUS Contrast-enhanced ultrasonography CI Confidence interval CT Computed tomography," *Eur Radiol*, vol. 27, pp. 2161–2169, 2017.

[13] S. Laurent *et al.*, "Expert consensus document on arterial stiffness: methodological issues and clinical applications," *Eur. Heart J.*, vol. 27, no. 21, pp. 2588–2605, Sep. 2006.

[14] K. Fujikura *et al.*, "A Novel Noninvasive Technique for Pulse-Wave Imaging and Characterization of Clinically-Significant Vascular Mechanical Properties *In Vivo*," *Ultrason. Imaging*, vol. 29, no. 3, pp. 137–154, Jul. 2007.

[15] R. X. Li, J. Luo, S. K. Balaram, F. A. Chaudhry, D. Shahmirzadi, and E. E. Konofagou, "Pulse wave imaging in normal, hypertensive and aneurysmal human aortas *in vivo* : a feasibility study," *Phys. Med. Biol.*, vol. 58, no. 13, pp. 4549–4562, Jul. 2013.

[16] Jianwen Luo, K. Fujikura, L. S. Tyrie, M. D. Tilson, and E. E. Konofagou, "Pulse Wave Imaging of Normal and Aneurysmal Abdominal Aortas *In Vivo*," *IEEE Trans. Med. Imaging*, vol. 28, no. 4, pp. 477–486, Apr. 2009.

[17] I. Z. Apostolakis, M. D. J. McGarry, E. A. Bunting, and E. E. Konofagou, "Pulse wave imaging using coherent compounding in a phantom and *in vivo*," *Phys. Med. Biol.*, vol. 62, no. 5, pp. 1700–1730, Mar. 2017.

[18] I.-Z. Apostolakis, P. Nauleau, C. Papadacci, M. D. McGarry, and E. E. Konofagou, "Feasibility and Validation of 4-D Pulse Wave Imaging in Phantoms and In Vivo," *IEEE Trans. Ultrason. Ferroelectr. Freq. Control*, vol. 64, no. 9, pp. 1305–1317, Sep. 2017.

[19] P. Nauleau, I. Apostolakis, M. McGarry, and E. Konofagou, "Cross-correlation analysis of pulse wave propagation in arteries: In vitro validation and in vivo feasibility," *Phys. Med. Biol.*, vol. 63, no. 11, p. 115006, May 2018.

[20] G. M. Karageorgos, I. Z. Apostolakis, P. Nauleau, R. Weber, and E. E. Konofagou, "Automated Spatial Mechanical Inhomogeneity Detection and Arterial Wall Characterization in Human Atherosclerotic Carotid Arteries In-Vivo," in *2018 IEEE International Ultrasonics Symposium (IUS)*, 2018, pp. 1–9.

[21] I. Z. Apostolakis, S. D. Nandlall, and E. E. Konofagou, "Piecewise Pulse Wave Imaging (pPWI) for Detection and Monitoring of Focal Vascular Disease in Murine Aortas and Carotids In Vivo," *IEEE Trans. Med. Imaging*, vol. 35, no. 1, pp. 13–28, Jan. 2016.

[22] I. Z. Apostolakis, P. Karageorgos, Grigorios M. Nauleau, S. D. Nandlall, and E. E. Konofagou, "Adaptive Pulse Wave Imaging: automated spatial vessel wall inhomogeneity detection in phantoms and in-vivo," *Trans. Med. Imaging*, no. (Under review), 2019.

[23] S. D. Nandlall, M. P. Goldklang, A. Kalashian, N. A. Dangra, J. M. D'Armiento, and E. E. Konofagou, "Monitoring and staging abdominal aortic aneurysm disease with pulse wave imaging.," *Ultrasound Med. Biol.*, vol. 40, no. 10, pp. 2404–14, Oct. 2014.

[24] R. X. Li *et al.*, "Pulse Wave Imaging in Carotid Artery Stenosis Human Patients in Vivo.," *Ultrasound Med. Biol.*, vol. 0, no. 0, Nov. 2018.

[25] G. Pasterkamp, D. P. . de Kleijn, and C. Borst, "Arterial remodeling in atherosclerosis, restenosis and after alteration of blood flow: potential mechanisms and clinical implications," *Cardiovasc. Res.*, vol. 45, no. 4, pp. 843–852, Mar. 2000.

[26] C. K. Zarins, D. P. Giddens, B. K. Bharadvaj, V. S. Sottiurai, R. F. Mabon, and S. Glagov, "Carotid bifurcation atherosclerosis. Quantitative correlation of plaque localization with flow velocity profiles and wall shear stress.," *Circ. Res.*, vol. 53, no. 4, pp. 502–14, Oct. 1983.

[27] K. V Ramnarine, D. K. Nassiri, P. R. Hoskins, and J. Lubbers, "Validation of a New Blood-Mimicking Fluid for Use in Doppler Flow Test Objects," *Ultrasound Med. Biol.*, vol. 24, no. 3, pp. 451–459, Mar. 1998.

[28] S. A. Maas, B. J. Ellis, G. A. Ateshian, and J. A. Weiss, "FEBio: Finite Elements for Biomechanics," *J. Biomech. Eng.*, vol. 134, no. 1, Feb. 2012.

[29] I. Zacharias, "Physics in Medicine & Biology Pulse wave imaging using coherent compounding in a phantom and in vivo," *Phys. Med. Biol*, vol. 62, 2017.

[30] C. Demene *et al.*, "Spatiotemporal Clutter Filtering of Ultrafast Ultrasound Data Highly Increases Doppler and fUltrasound Sensitivity," *IEEE Trans. Med. Imaging*, vol. 34, no. 11, pp. 2271–2285, Nov. 2015.

[31] Wei-Ning Lee, C. M. Ingrassia, S. D. Fung-Kee-Fung, K. D. Costa, J. W. Holmes, and E. E. Konofagou, "Theoretical Quality Assessment of Myocardial Elastography with In Vivo Validation," *IEEE Trans. Ultrason. Ferroelectr. Freq. Control*, vol. 54, no. 11, pp. 2233–2245, Nov. 2007.

[32] Y. I. Cho and K. R. Kensey, "Effects of the non-Newtonian viscosity of blood on flows in a diseased arterial vessel. Part 1: Steady flows.," *Biorheology*, vol. 28, no. 3–4, pp. 241–62, 1991.